

Synthesis and magnetic characteristics of core-shell Fe₃O₄ nano-particles with highly efficient performances

XINYUAN YUWEN, XIAORUI HU, HAIHONG YAN, R. REN*, YILIN WANG, FUHAI ZHAO, XUNCHAO CHU
Department of Optics Information, MOE KLNSMC Mechanical, Physics, 710049, Xian Jiaotong University, Xian 712000, P.R. China

The core-shell Fe₃O₄@SiO₂ and Fe₃O₄@SiO₂@TiO₂ nanoparticles were prepared by the chemical co-precipitation method and chemical conversion process, and characterized by X-ray diffraction (XRD), transmission electron microscopy (TEM), saturated magnetization (VSM), FTIR and adsorbent spectrum, and UV-visible spectroscopy. VSM indicated the Fe₃O₄@SiO₂ nano-spheres had saturated magnetization of 33.5 emu/g and coercive force of 85 Oe. XRD patterns 2θ peaks of Fe₃O₄ matched well with lattice planes of the face-centered cubic lattice of JCPDS Card. The Fe₃O₄@SiO₂ diffraction angles of 30.28°, 35.58°, 43.24°, 57.26°, and 62.71° corresponded to SiO₂(220), (311), (400), (511), and (440) crystal faces, respectively. Compared to the room temperature spectrum, FTIR spectra confirmed the peaks at 1325 and 1152 cm⁻¹ were ascribed to O=S=O stretching vibrations. The result may be attributed to that the surface-modified Fe₃O₄ and the utilization of visible light and hinder the recombination process.

(Received June 11, 2020; accepted November 25, 2020)

Keywords: Magnetic nano-structures, Magnetic core-shell, Synthesis, Heterostructure

1. Introduction

This Fe₃O₄ nanoparticles are widely used in magnetic imaging biomedicine [1], electromagnetic wave absorption [2] heavy metal ions removal [3], image diagnosis, and biomedicine fields. This growing interest of Fe₃O₄ is due to its characteristics such as strong magnetism, long durability, good biocompatibility, low toxicity and low cost [4, 5]. Nano- magnetic core-shell Fe₃O₄ has shown their tremendous potential in MR imaging, drug delivery, bio-molecule tagging and capturing inorganic or organic pollutants from water. Recently, the rapid advance of nano-magnetic Fe₃O₄ materials and nano-technology has brought new opportunities for water treatment. Nevertheless, Because of their easy suspension in water, it is quite difficult to remove these nanomaterials from large volumes of water, which limits their practical application. An effective strategy to solve this problem is to embed magnetic iron oxides to form magnetic nanocomposites, which provides a convenient tool for exploring magnetic separation techniques as a result of their unique magnetic response [6, 24–29].

Magnetic Fe₃O₄ nano -particles have been widely used in magnetic targeting, image diagnosis, drug carrier, magnetic heat treatment and magnetic separation due to its inherent magnetic and surface effect [12-17]. Also, silicate materials have been used as adsorbents by many researchers for removal of some toxic metal ions [18–23]. Titanium dioxide nanoparticles as photocatalyst have the

role of degradation of toxic heavy metal pollutants. Particularly detailed study of U(VI) adsorption on various nanoscale adsorbents like hollow SiO₂ nano-spheres functionalized with amidoxime [9], nanoscale zero valent iron on activated charcoal [7], diamine functionalized hollow silica nano-spheres [9], hydrous TiO₂ [14] and magnetic oxide have been reported importantly [8,10,11].

In the present work, we report the synthesis of Fe₃O₄@SiO₂, Fe₃O₄@PZS@TiO₂, and Fe₃O₄@SiO₂@TiO₂ nano-particles with well-defined core-shell nanostructure. Fe₃O₄ subnano-spheres were obtained by the chemical co-precipitation method via a chemical conversion route using chemical template. The as-prepared Fe₃O₄@ SiO₂ @TiO₂ micro-spheres were characterized, which consists of a magnetite core and a magnesium silicate shell. The nano-composites have been measured by X-ray Powder Diffraction (XRD), HR-TEM, FTIR spectroscopy, and VSM. The Fe₃O₄ nano-particles with well-defined core-shell nanostructure obtained not only show magnetism but also have enhanced conductive, optical, catalytic and biological properties nanoparticles compared to individual component materials.

2. Experimental section

2.1. Preparing of Fe₃O₄@PZS nano-spheres

Mono-dispersed nano-spheres of various average sizes

were synthesized according to our experiment. Typically, Triton X-100 (1.5 mL, $0.98 \text{ g}\cdot\text{mL}^{-1}$) was added to NaOH aqueous solution (250.0 mL, 1.0M) contained in an erlenmeyer flask for the synthesis of 20 nm Fe_3O_4 nano-particles. After vigorous stirring for 1 h, $\text{FeCl}_3\cdot 6\text{H}_2\text{O}$ (0.71g) and $\text{FeCl}_2\cdot 4\text{H}_2\text{O}$ (0.71 g, 1:1, by mole) were dissolved in deionized water uniformly, which was added to the above solution slowly with vigorous stirring at 80°C for 0.5h. Furthermore, it was sealed and heated at 200°C for 12h before cooling to room temperature. The Fe_3O_4 powders were washed and extracted by centrifuge separation using acetone at a speed of 6000 rpm for 15 min. The black precipitate was washed for two times using with anhydrous ethanol and deionized water using a speed of 6000 rpm for 15 min. Then, the black nano-spheres Fe_3O_4 were dried in a vacuum oven.

The chemical Iron(III) chloride hexahydrate ($\text{FeCl}_3\cdot 6\text{H}_2\text{O}$) and Iron(II) chloride tetrahydrate ($\text{FeCl}_2\cdot 4\text{H}_2\text{O}$) were purchased from Chemical Reagent Co.Ltd. The t-Oct-C₆H₄-(OCH₂CH₂)_xOH, (x=9-10, Triton X-100), hexachloro-cyclotriphosphazene (HCCP), tetrahydrofuran (THF), anhydrous ethanol, triethylamine (TEA), 4,4'-sulfonyldiphenol (BPS), chloroauric acid (HAuCl_4), sodium borohydride (NaBH_4), Tetraethyl orthosilicate (TEOS), sodium citrate (Na_3Ct), acetic acid, titanium tetrabutoxide (TBOT), Sodium hydroxide (NaOH) were used with analytical purity from Chemical Reagent Co. Ltd. All reagents were used without further treatment.

Thus, Fe_3O_4 nanoparticles (0.4g) and HCCP (1.6g) were dissolved in a mixed solution of THF (81.0 mL), anhydrous ethanol (9.0 mL) and TEA (20.0 mL) by sonication for 20 min, followed by the addition of BPS (3.6 g) sequentially. The mixture reacted for 6h at room temperature under a continuous sonication. The resultant precipitate was washed with THF and anhydrous ethanol, and it was dried in the vacuum.

Moreover, 100 mg of the prepared Fe_3O_4 @PZS nano-particles were dispersed in a mixture of 180 mL of ethanol and 50 mL of deionized water by ultra-sonication for 10 min. Then acetic acid (10 mL), H_2O (3 mL) and anhydrous ethanol (30 mL) were dissolved in beaker and added in drops to the above solution with vigorous stirring for 40 min, followed by heating the solution under reflux at 85°C for 90 min. The resulting products were washed with acetone, deionized water, and anhydrous ethanol by magnetic decantation three times and dried in the vacuum. The solid products were collected using an external magnetic field, rinsed with deionized water, ethanol and dried in a vacuum oven.

2.2. Fabricated Fe_3O_4 @ SiO_2 nano-spheres

100 mg of the prepared Fe_3O_4 @PZS nano-particles was dispersed in a mixture of 30 mL ethanol and 50 mL deionized water by ultrasonication for 15 min. Then, under

continuous mechanical stirring, 24 mL ammonia solution (25%) and 1.8 mL TEOS were added to mixture sample dropwise. The reaction was allowed to proceed at 40°C for 6 h. The resulting products were collected and washed, and then refluxed under continuous mechanical stirring in 120 mL ethanol at 80°C for 12 h. The solid products were collected using an external magnetic field, rinsed with deionized water, ethanol and dried in a vacuum oven at 60°C for 4 h.

2.3. Synthesis of Fe_3O_4 @ SiO_2 @ TiO_2 nano-spheres

The core-shell Fe_3O_4 @ SiO_2 @ TiO_2 nano-spheres were synthesized by the previously reported method. Briefly, the above Fe_3O_4 @ SiO_2 solution (0.15g) was mixed with ethanol (30 mL), deionized water (3 mL), and HPC (0.05 g) under vigorous stirring for 40 min. Then, 0.2 mL TBOT dissolved in ethanol (5 mL) was added dropwise, followed by heating the solution under reflux at 85°C for 90 min. Finally, the resulting products were washed with ethanol four times by magnetic decantation and dried at 60°C for 6 h under vacuum.

2.4. Measurement method

Transmission electron microscopy (TEM) images, high-resolution TEM (HRTEM), and EDS spectroscopy were performed on a JEOL TEM-2100 operating transmission electron microscope equipped with a post-column Gatan imaging filter (GIF-Tridium) at an acceleration voltage of 200 kV. Powder X-ray diffraction (XRD) measurements were carried out using a Bruker D8 Advance X-ray diffractometer with Ni-filtered Cu-K α radiation (40 kV, 40 mA). Fourier transform infrared (FTIR) spectroscopy was recorded on Bruker tensor 27 spectrometer using KBr pellets. Magnetic properties were determined with Lakeshore 665 vibrating sample magnetometry (VSM). Photographs were taken with a digital camera (PowerShot SX210 IS, Canon, Japan). UV-vis absorption spectrum was obtained by spectrophotometer at room temperature. The Brunauer-Emmett Teller (BET) method was utilized to calculate the specific surface areas using adsorption data in a relative pressure range from 0.05 to 0.25. Fluorescence emission spectrum and excitation spectra were obtained by Edinburch instruments FSL 980 S2S2 -STM 152 spectrophotometer in the UV-VIS-NIR spectral range at low temperature.

3. Results and discussion

3.1. Procedure

The mechanism of fabricating highly cross-linked PZS

products by S_N2 reaction between HCCP and BPS, as well as the preparation procedure of Fe₃O₄@PZS@TiO₂ nano-spheres are presented in Fig. 1. First, Fe₃O₄ nano-spheres were obtained by the chemical co-precipitation of FeCl₃•6H₂O and FeCl₂•4H₂O. Then, Fe₃O₄@PZS nano-particles were achieved by coating the

highly cross-linked PZS obtained by the poly-condensation of comonomers HCCP and BPS. Finally, SiO₂ shell was coated by isopropyl alcohol and ammonia solution using the Stöber method to obtain Fe₃O₄@SiO₂ core-shell micro-spheres, and TiO₂ shell was created by the hydrolysis of titanium tetrabutoxide (TBOT).

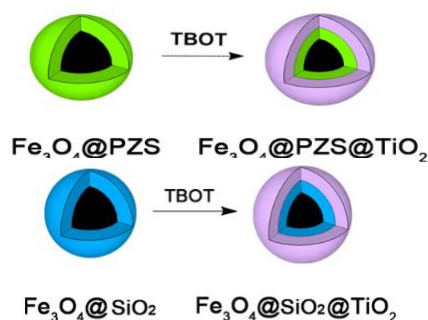


Fig. 1. Preparation procedure of Fe₃O₄@PZS@TiO₂ nanostructure. Mechanism of fabricating highly cross-linked PZS products by S_N2 reaction between HCCP and BPS (color online)

3.2. TEM properties

The morphological structure of Fe₃O₄, Fe₃O₄@PZS@TiO₂ (a) and Fe₃O₄@SiO₂ nano-spheres (b) were investigated by high resolution transmission electron

microscopy JEOL TEM-2100 (HR-TEM). Fig. 2 shows the well obtained core-shell Fe₃O₄@PZS@TiO₂ nano-composites with the average size of about 15 nm. The microscopy of Fe₃O₄ crystal lattice structure is measured as shown in Fig. 2.

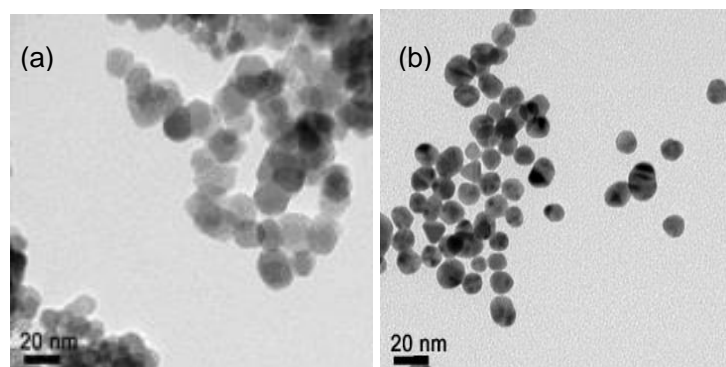


Fig. 2. The TEM images of (a) Fe₃O₄@PZS@TiO₂ nanoparticles and (b) Fe₃O₄@SiO₂ nanoparticles

3.3. XRD characteristics

The crystallographic structure and phase purity of the synthesized products are identified by XRD. Fig. 3 indicated XRD patterns of Fe₃O₄, Fe₃O₄@SiO₂ nano-particles. The XRD patterns were recorded in a reflection mode (Cu K α radiation) on a Bruker D8 Advance X-ray diffractometer. The five characteristic peaks of Fig. 3 ($2\theta=30.28, 35.58, 43.24, 57.26, 62.71$) corresponded to the (220), (311), (400), (511), and (440) lattice planes of the face-centered cubic lattice of Fe₃O₄ (JCPDS Card No.19-0629), while the peaks of Fe₃O₄ were also observed in Fe₃O₄@PZS illustrating that the phases of the surface modified Fe₃O₄ were not changed. As for the

Fe₃O₄@PZS@Au nano-particles, besides the peaks of Fe₃O₄, four additional peaks positioned at 2θ values of 38.37, 44.32, 64.65, and 77.71 matched well with the (111), (200), (220), and (311) lattice planes of the face-centered cubic lattice of Au (JCPDS Card No.04-0784), which showed that the presence of Au in Fe₃O₄@PZS@Au nano-particles. The five characteristic peaks of Fe₃O₄ were observed in Fe₃O₄@SiO₂. After coating with the TiO₂ layer and air annealing, we tested crystallization and phase composition of TiO₂ nano-spheres. The three characteristic peaks ($2\theta=25.3^\circ, 37.8^\circ, 48.0^\circ$) corresponded to TiO₂ anatase phase (101), (004) and (200) lattice planes of the cubic lattice of Fe₃O₄.

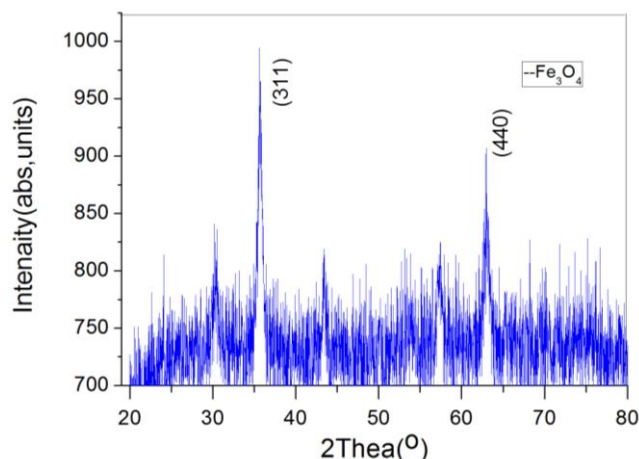


Fig. 3. XRD patterns of Fe_3O_4 nanoparticles

3.4. VSM Magnetic performances

Fig. 4 shows the hysteresis loops of the dried $\text{Fe}_3\text{O}_4@/\text{SiO}_2$ nano-particles cycling the field between -7500 Oe to 7500 Oe at room temperature. Curve is the hysteresis loop of $\text{Fe}_3\text{O}_4 @ \text{SiO}_2$ nano-spheres, the saturated magnetization is 33.5 emu/g, coercive force of 85 Oe. It indicated that Fe_3O_4 remained strong magnetic structure, after the Fe_3O_4 nano-particles were carried out on surface modification of organic polymer and inorganic nano-particles. The hysteresis loops of the dried $\text{Fe}_3\text{O}_4@/\text{SiO}_2$ nano-particles display good performances at room temperature cycling the field between -7500 Oe to 7500 Oe.

Fig. 5 shows that nano $\text{Fe}_3\text{O}_4@/\text{SiO}_2$ nano-spheres are dispersed in deionized water. The liquid came in light brown liquid as shown in Fig. 5 on the right. The magnet particles can quickly gather under a plus magnet. If we remove the magnet and shake slightly, the $\text{Fe}_3\text{O}_4 @ \text{SiO}_2$ can spread out again. Using organic polymer and inorganic nanoparticles surface modified, the nanoparticles $\text{Fe}_3\text{O}_4 @ \text{PZS}$, and $\text{Fe}_3\text{O}_4@/\text{SiO}_2@/\text{TiO}_2$ also displayed strong magnetic properties and stability in the same way.

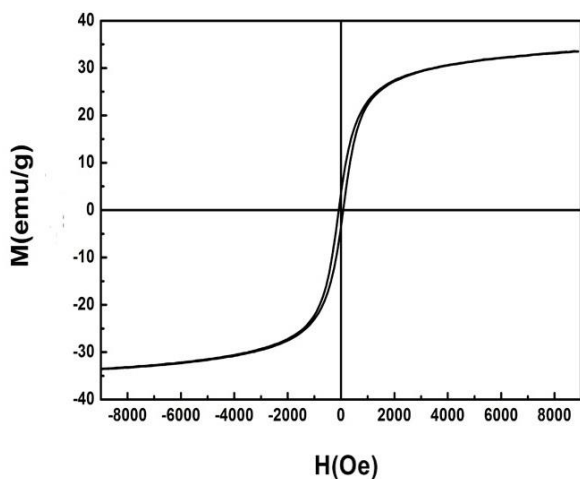


Fig. 4. The magnetization curve of $\text{Fe}_3\text{O}_4@/\text{SiO}_2$ nano-particles at room temperature cycling the field between -7500 Oe to 7500 Oe

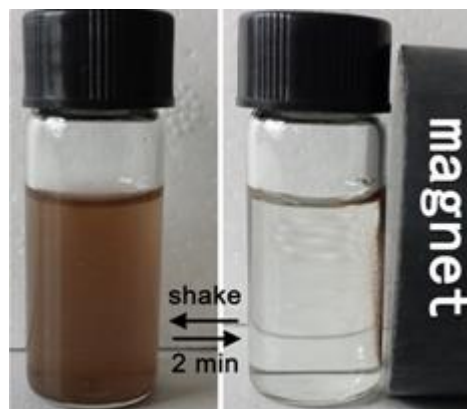


Fig. 5. Magnetic nanoparticles $\text{Fe}_3\text{O}_4@/\text{SiO}_2$ absorbed by magnets

3.5. FTIR and single emission monochromator Fluorescence spectrometer performances

Fig. 6 shows FTIR spectra of $\text{Fe}_3\text{O}_4@/\text{PZS}$ nanoparticles. The peaks at 1325 and 1152 cm^{-1} (peak 1 and 2) were ascribed to the $\text{O}=\text{S}=\text{O}$ stretching vibrations of the BPS, and the peaks at 1489 and 1587 cm^{-1} (peak 3 and 4) were assigned to the $\text{C}=\text{C}$ stretching vibrations of the BPS. The peak at 1185 cm^{-1} (peak 5) was associated with the $\text{P}=\text{N}$ stretching vibration of the HCCP shown in Fig. 7. Furthermore, the peak at 941 cm^{-1} (peak 6) was ascribed to the $\text{P}-\text{O}-\text{Ar}$ band, which was an obvious evidence of the existent of PZS obtained by the comonomers HCCP and BPS. For pure magnetic Fe_3O_4 , the vibrational band Fe_3O_4 at around 586 cm^{-1} is related to the ν ($\text{Fe}-\text{O}$) lattice vibration. The silica coated magnetite sample shows two weak absorption bands at 804 cm^{-1} and 950 cm^{-1} , and a significant characteristic absorption band at 1099 cm^{-1} , corresponding to the stretching vibrations of ν ($\text{Si}-\text{O}-\text{Fe}$), ν ($\text{Si}-\text{OH}$) and ν ($\text{Si}-\text{O}-\text{Si}$), respectively. These results indicate that SiO_2 is deposited on the surface of Fe_3O_4 nano-spheres and $\text{Fe}_3\text{O}_4@/\text{PZS}$ core-shell nano-spheres shown in Fig. 7.

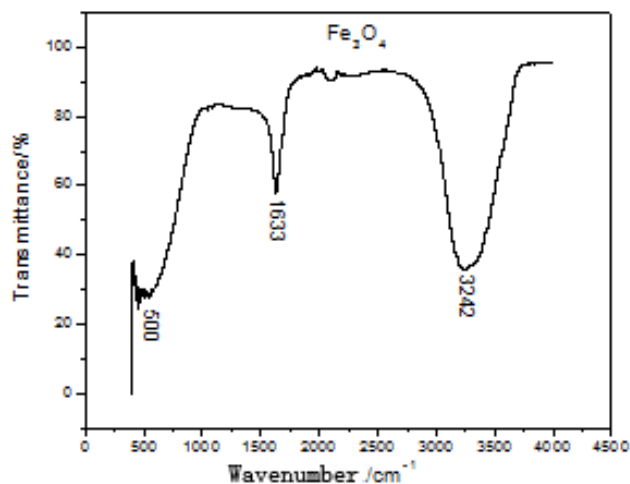


Fig. 6. FTIR spectra of Fe_3O_4 nanoparticles

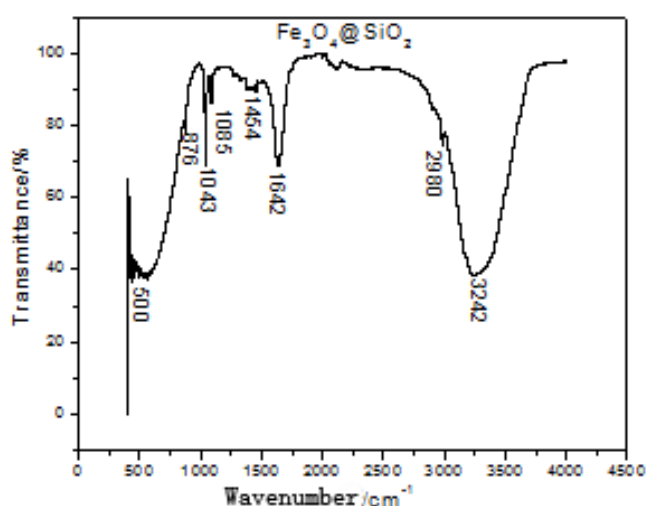


Fig. 7. FTIR spectra of Fe₃O₄@SiO₂ nano-particles

When these images are combined with line scanning profiles, the core-shell structure of a Fe₃O₄ core and TiO₂ nanosheet shells can be clearly observed. From the EDS, XRD, and HRTEM results, it can be confirmed that hierarchical Fe₃O₄@TiO₂ core-shell nano-spheres have been successfully synthesized.

The magnetic nanoparticles Fe₃O₄ coated TiO₂ show some weak emission bands at 393, 437, 458, 546, 569, 594, 617, 642 nm and a significant emission band characteristic at 666 nm corresponding to the stretching vibrations of $\nu(\text{Ti-O-Fe})$, $\nu(\text{Ti-OH})$ and $\nu(\text{Ti-O-Ti})$, respectively. The measured results suggested that the obtained magnetic hetero-structure nano-crystals could be a promising catalyst in the photo-Fenton process.

4. Conclusion

In summary, the core-shell nano-particles Fe₃O₄@SiO₂, Fe₃O₄@PZS@TiO₂ and Fe₃O₄@SiO₂@TiO₂ with well-defined core-shell nano-structures have been successfully synthesized by coating the Fe₃O₄@PZS nano-structures with SiO₂ and TiO₂ shells, respectively. The Fe₃O₄@SiO₂, Fe₃O₄@PZS@TiO₂ and Fe₃O₄@SiO₂@TiO₂ core-shell could indicate better super-paramagnetism even though Fe₃O₄ nano-particles were encapsulated in SiO₂, and TiO₂ shells. In addition, the Fe₃O₄@SiO₂, Fe₃O₄@PZS@TiO₂ and Fe₃O₄@SiO₂@TiO₂ with well-defined core-shell nanostructure not only have obtained the magnetism of Fe₃O₄ but also have FTIR spectra fluorescence, enhanced conductive, optical, catalytic and biological properties of PZS, SiO₂, and TiO₂ core-shell nano-structures compared to their individual single component materials. The results suggested that the as-obtained magnetic hetero-structure nano-crystals could be a promising catalyst in the photo-Fenton process. The Fe₃O₄ magnetoelectricity

properties are due to the strong hybridization of the unoccupied iron 3d states with the oxygen 2p at the tetrahedral site.

Acknowledgements

The work was supported by the National Natural Science Foundation of China Nos 61574115, and NSFC Projects of International Cooperation and Exchanges of China 2018, 2019, ShaanXi Natural Science Basic Research Plan in Shaanxi Province of China (2020JM080), the xjtu Fundamental Research Funds for the Central Universities (zdyf2017014).

References

- [1] Lazhen Shen, Yongsheng Qiao, Yong Guo, *Optoelectron. Adv. Mat.* **7**(7-8), 525 (2013).
- [2] Xian Jian, Xiangyun Xiao, Longjiang Deng, *ACS Applied Materials & Interfaces*, **10**(11), 9369 (2018).
- [3] R. Kumar, R. K. Singh, A. H. Vaz, J. Roger, J. N. Pons, D. Geldwerth, *ACS Applied Materials & Interfaces* **9**(10), 8880 (2017).
- [4] S. H. Sun, S. X. Li, *J. Am. Chem. Soc.* **126**, 273 (2004).
- [5] Gul G. Celik, *Optoelectron. Adv. Mat.* **12**(1-2), 112 (2018).
- [6] J. M. Nam, C. S. Thaxton, C. A. Mirkin, *Science* **301**, 1884 (2003).
- [7] J. H. Gao, G. L. Liang, B. Zhang, Y. Kuang, X. X. Zhang, B. Xu, *J. Am. Chem. Soc.* **129**, 1428 (2007).
- [8] A. Nemat, S. Shadpour, H. Khalafbeygi, M. Barkhi, *Synth. React. Inorg. M* **44**, 1161 (2014).
- [9] Q. L. Fang, S. H. Xuan, W. Q. Jiang, X. L. Gong, *Adv. Funct. Mater.* **21**, 1902 (2011).
- [10] P. Pouponneau, J. C. Leroux, G. Soulez et al., *Biomaterials* **32**(13), 3481 (2011).
- [11] X. Q. Liu, V. Novosad, E. A. Rozhkova et al., *IEEE Tran. Magn.* **43**(6), 2462 (2007).
- [12] Li Na, G. W. Huang, Y. Q. Li, *ACS Applied Materials & Interfaces* **9**(3), 2973 (2017).
- [13] F. Yang, P. Ghen, W. He, Bubble, *Small* **6**(12), 1300 (2010).
- [14] R. L. Zhou, D. D. Li, B. Y. Qu, X. R. Sun, B. Zhang, X. C. Zeng, *ACS Applied Materials & Interfaces* **40**(8), 27403 (2016).
- [15] X. F. Lu, H. Mao, D. M. Chao, W. J. Zhang, Y. Wei, *J. Solid State Chem.* **179**, 26092615 (2006).
- [16] W. L. Chiang, G. J. Ke, Z. X. Liao, S. Y. Chen, F. R. Chen, C. Y. Tsai, Y. N. Xia, H. W. Sung, *Small* **8**(23), 3584 (2012).
- [17] R. Valenzuela, M. C. Fuente, C. Parra, J. Baeza, N. Duran, S. K. Sharma, M. Knobel, J. Freer, *J. Alloy Compound.* **488**, 227 (2009).
- [18] L. Y. Wang, J. Luo, Q. Fan, M. Suzuki, I. S. Suzuki, M. H. Engelhard, Y. H. Lin, N. Kim, J. Q. Wang, C. J.

- Zhong, *J Phys. Chem. B* **109**, 21593 (2005).
- [19] C. L. Zhu, M. L. Zhang, Y. J. Qiao, G. Xiao, F. Zhang, Y. J. Chen, *J. Phys. Chem. C* **114**, 16229 (2010).
- [20] S. H. Xuan, W. Q. Jiang, X. L. Gong, Y. Hu, Z. Y. Chen, *J. Phys. Chem. C* **113**, 553 (2009).
- [21] L. Zhou, C. Gao, W. J. Xu, *Langmuir* **26**, 11217 (2010).
- [22] S. H. Xuan, Y. X. J. Wang, J. C. Yu, K. C. F. Leung, *Langmuir* **25**, 11835 (2009).
- [23] Y. H. Fan, C. H. Ma, W. G. Li, Y. S. Yin, *Mat. Sci. Semicon. Proc.* **15**, 582 (2012).
- [24] L. Zhu, Y. Y. Xu, W. Z. Yuan, J. Y. Xi, X. B. Huang, X. Z. Tang, S. X. Zheng, *Adv. Mater.* **18**, 2997 (2006).
- [25] M. H. Wang, J. W. Fu, D. D. Huang, C. Zhang, Q. Xu, *Nanoscale* **5**, 7913 (2013).
- [26] Wu Tong, Y. Liu, X. Zeng, *ACS Applied Materials & Interfaces* **8**(11), 7370 (2016).
- [27] X. Jian, B. Wu, Wei Yufeng, *ACS Applied Materials & Interfaces* **8**(9), 6101 (2016).
- [28] J. L. Lyon, D. A. Fleming, M. B. Stone, P. Schiffer, M. E. Williams, *Nano Lett.* **4**, 719 (2004).
- [29] R. Kumar, R. K. Singh, A. Vaz, *ACS Applied Materials & Interfaces* **9**(10), 8880 (2017).

*Corresponding author: ren@mail.xjtu.edu.cn